Title

DNA and IκBα Both Induce Long-Range Conformational Changes in NFκB

Journal

Journal of Molecular Biology, 429(7)

ISSN

0022-2836

Authors

Ramsey, Kristen M
Dembinski, Holly E
Chen, Wei
et al.

Publication Date

2017-04-01

DOI

10.1016/j.jmb.2017.02.017

Peer reviewed

HHS Public Access

Author manuscript

J Mol Biol. Author manuscript; available in PMC 2018 April 07.

Published in final edited form as:

J Mol Biol. 2017 April 07; 429(7): 999–1008. doi:10.1016/j.jmb.2017.02.017.

DNA and IκBα both induce long range conformational changes in NFκB

Kristen M. Ramsey[1], **Holly E. Dembinski**[1], **Wei Chen**, **Clarisse G. Ricci**, and **Elizabeth A. Komives**[*]

Department of Chemistry and Biochemistry, University of California, San Diego, 9500 Gilman Drive, La Jolla, CA 92092-0378

Abstract

We recently discovered that IκBα enhances the rate of release of NFκB from DNA target sites in a process we have termed molecular stripping. Coarse-grained molecular dynamics simulations of the stripping pathway revealed two mechanisms for the enhanced release rate; the negatively charged PEST region of IκBα electrostatically repels the DNA, and binding of IκBα appears to twist the NFκB heterodimer so that DNA can no longer bind. Here we report amide hydrogen/deuterium exchange data that reveals long-range allosteric changes in the NFκB (RelA-p50) heterodimer induced by DNA or IκBα binding. The data suggest that the two immunoglobulin-like subdomains of each Rel-homology region, which are connected by a flexible linker in the heterodimer, communicate in such a way that when DNA binds to the N-terminal DNA binding domains, the nuclear localization signal becomes more highly exchanging. Conversely, when IκBα binds to the dimerization domains, amide exchange throughout the DNA binding domains is decreased as if the entire domain is becoming globally stabilized. The results help understand how the subtle mechanism of molecular stripping actually occurs.

Graphical abstract

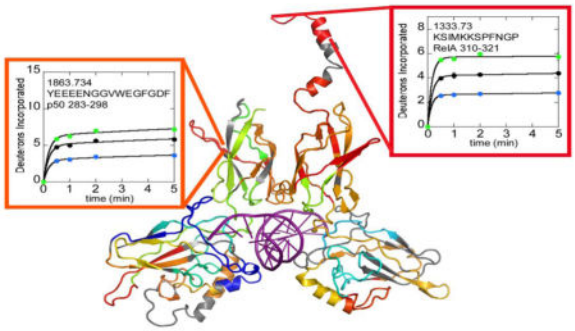

[*]Corresponding author: Elizabeth A. Komives, Department of Chemistry and Biochemistry, University of California, San Diego, 9500 Gilman Drive, La Jolla, CA 92092-0378, Ph: (858) 534-3058, ekomives@ucsd.edu.

[1]These authors contributed equally

Introduction

The nuclear factor kappa B (NFκB) family of transcription factors responds to a large number of extracellular stress stimuli, including factors controlling inflammation and the immune response [1,2,3]. Dysregulation of NFκB results in numerous disease states, particularly cancer [1,4,5]. NFκB is a member of the Rel homology domain-containing (RHD) family and Pfam has 887 sequences for which some 75 structures have been determined. The RHD is composed of two immunoglobulin-like (Ig-like) beta barrel subdomains connected by a flexible linker. Utilizing mostly irregular loops, both Ig-like subdomains engage the DNA major groove. The N-terminal Ig-like domain is typically referred to as the DNA-binding domain due to its large surface engaged in DNA-binding. The C-terminal Ig-like domain is responsible for dimerization and is therefore referred to as the dimerization domain.

The IκB family of inhibitors [6] bind in the groove formed between the two dimerization domains of NFκB dimers. The canonical NFκB (RelA-p50) heterodimer is held in the cytoplasm bound mainly to IκBα. Upon cellular stress, IKK phosphorylation followed by ubiquitylation allows proteasomal degradation of IκBα releasing NFκB and unmasking its nuclear localization sequence (NLS), allowing its translocation into the nucleus, where it binds to κB DNA sites, and upregulates gene expression. The promoter upstream of the IκBα gene is strongly up-regulated by NFκB resulting in synthesis of new IκBα (Figure 1). Free IκBα is very unstable, and is degraded by a non-ubiquitin-dependent mechanism with a half-life of seven minutes. In constrast, the NFκB-bound IκBα is stable for many hours due to the very high affinity of the NFκB-IκBα complex [7]. We previously showed that IκBα rapidly accelerates the dissociation of the canonical, and most abundant NFκB (RelA-p50) from DNA *in vitro* in a kinetically-driven process we have termed “molecular stripping” [8,9,10].

IκBα is a six-ankyrin repeat protein with a C-terminal PEST sequence. Previous work in our lab using hydrogen/deuterium exchange mass spectrometry (HDXMS) showed that the fifth and sixth ankyrin repeats (ARs) fold when IκBα binds to NFκB [11]. Simulations suggested that when IκBα binds to the NFκB-DNA complex during molecular stripping, the IκBα causes a twisting of the relative domain orientations within the NFκB(RelA-p50) heterodimer [10]. In order to investigate the mechanism of this proposed twisting, we set-out to perform HDXMS analyses on the NFκB portion of the complex. We present here the results of HDXMS analyses of free NFκB, DNA-bound NFκB, and IκBα-bound NFκB. The data reveal surprising long-range allosteric changes within the subdomains of NFκB upon DNA or IκBα binding.

Results

HDXMS of NFκB

HDXMS data was collected on a Synapt G2Si mass spectrometer, which provided 95% coverage of IκBα as compared to 72% coverage obtained previously using MALDI-TOF mass spectrometry [11]. For the experiments performed previously, NFκB was biotinylated and removed from the sample prior to pepsin digestion in order to decrease peptide overlap

during mass spectrometry. Here, we took advantage of the ion mobility capabilities of the Synapt, which effectively allowed for a third dimension of separation because the DynamX 3.0 software takes the mobility time into account for identification of deuterated peptides. Each peak in the mass spectrum could be unambiguously identified by its mass, its retention time, and its ion mobility to differentiate overlapping peaks. Therefore in these experiments, no removal of the partner protein was required. For IκBα, 109 peptides were identified as compared to 28 we analyzed previously [11]. Although we analyzed 109 peptides for IκBα, we realized that a subset of 61 peptides achieve maximal coverage and information content. The results of the newer data, which include complete coverage of AR5, confirmed previous results and were recently published [12]. Similarly, although 69 peptides for RelA and 83 peptides for p50 were analyzed, a subset of 17 peptides from RelA and 18 peptides from p50 that achieve maximal coverage and information content are presented here (Supplementary Figure 1). All of the overlapping peptides not presented here were fully analyzed, and no additional information was obtained from them.

HDXMS confirms the surface of NFκB that interacts with DNA or with IκBα

Crystal structures of DNA bound to NFκB (for example PDB code 1LE5) all show that DNA contacts the N-terminal DNA-binding domains and a loop in the dimerization domains of both RelA and p50. Consistent with the structural data, HDXMS revealed large decreases in exchange of RelA residues 23-34, m/z 1502.826; residues 77-99, m/z 2653.305 in the DNA-binding domain and residues 214-226, m/z 1531.804 in the dimerization domain. In p50, large decreases in exchange were observed in DNA-binding domain residues 43-55, m/z 1646.912; residues 56-86, m/z 3333.647; residues 97-121, m/z 2681.340; residues 135-151, m/z 1911.143; and in dimerization domain residues 269-279, m/z 1304.652 (Figure 2).

Crystal structures of IκBα with NFκB (RelA-p50) (PDB codes 1NFI and 1IKN) show an extensive (~4000 $Å^2$) interface between the dimerization domains of the NFκB subunits and IκBα [13,14]. Therefore it was expected that the regions of RelA and p50 that were contacting IκBα in these structures would show decreased amide exchange upon binding of IκBα. Indeed, p50 residues 249-265 (m/z=1821.895) and RelA residues 240-251 (m/z=1322.718) directly contact (at least one non-hydrogen atom is within 5Å) IκBα and show marked protection from exchange when bound to IκBα (Figure 3). An additional region of p50 (residues 328-250, m/z=2842.477) and two additional regions of RelA (residues 195-213, m/z=1877.895 and residues 214-226, m/z=1531.804) showed marked decreases in exchange but do not directly contact IκBα (closest non-hydrogen atom is >9Å away). These regions are adjacent to regions of the dimerization domains that directly contact IκBα (Figure 3).

DNA binding induces both increases and decreases in exchange in the NFκB Rel Homology domains

In addition to the decreases in exchange expected from formation of the DNA-NFκB interface, both increases and decreases in exchange were observed in both the DNA-binding domains and dimerization domains of the NFκB Rel Holomogy domains far from the DNA-binding interface (Figure 4 and Supplementary Figure 1). Of particular interest are RelA

residues 227-239, m/z 1474.675 and the corresponding structural region of p50, residues 283-298, m/z 1863.734. These strand-loop-strand motifs protrude from the dimerization domains of NFκB and exchange substantially more in the DNA-bound NFκB as compared to the free protein. In addition, Rel A residues 310-321, m/z 1333.730, which correspond to the helical region containing the nuclear localization signal (NLS), also exchanged substantially more in the DNA-bound protein (Figure 4). It is interesting to note that all of the regions that exchanged more in the DNA-bound protein as compared to free NFκB were protected from exchange by IκBα binding (data for all three states are shown in Figure 4).

IκBα binding induces global decreases in exchange in the NFκB DNA-binding domains far from the IκBα binding interface

In the structures of the NFκB-IκBα complex (PDB codes 1NFI and 1IKN), no direct contacts are observed between the IκBα and the N-terminal DNA-binding domains of NFκB. We were therefore very surprised to observe marked decreases in exchange throughout the DNA-binding domains upon IκBα binding. The HDXMS data covered 79% of the RelA sequence and significantly decreased exchange was observed for every single peptide throughout the RelA DNA-binding domain upon IκBα binding (Figure 5, Supplementary Figure 1). In p50, 92% of the sequence was covered, and again decreased exchange was observed in every single region of the p50 DNA-binding domain upon IκBα binding except for two regions, residues 87-96 and residues 152-158 which did not exchange significantly under any conditions (Figure 3, Supplementary Figure 1).

Equilibrium unfolding experiments indicate that the “folding” of the NFκB (RelA-p50) DNA-binding domains is consistent with global stabilization of NFκB upon IκBα binding

Given that NFκB is a transcription factor, it would be expected that DNA binding would stabilize the fold. We therefore performed circular dichroism measurements monitoring the signal at 225nm. We previously published full scan CD data for IκBα, NFκB (dimerization domain constructs), and the NFκB-IκBα complex [15]. Here, we performed thermal melting of free NFκB and its complexes. The melting temperature of NFκB increased from 55°C to 65°C upon binding the DNA hairpin containing a single κB site (Figure 6). Remarkably, however, attempts to melt the NFκB-IκBα complex were unsuccessful showing that IκBα stabilizes NFκB to thermal challenge by at least 30°C. This result is consistent with the global decrease in amide exchange observed upon IκBα binding to NFκB and also with the very long intracellular half-life of NFκB when it is bound to IκBα [7].

Comparison of IκBα-bound to full-length NFκB with DNA-binding domain deletion NFκB constructs reveals key allosteric sites in the NFκB dimerization domains

To further probe the long-range allostery between the DNA-binding domains and the dimerization domains, we took advantage of the fact that IκBα binds to NFκB primarily at the dimerization domains. Indeed, the binding affinity of IκBα to the DNA-binding domain deletion construct is only 10-fold weaker than to full-length NFκB (300 pM vs 30 pM) [16]. The deuterium uptake into full-length NFκB in complex with IκBα was compared to the deuterium uptake into the DNA-binding domain deletion NFκB construct in complex with IκBα. Although most of the dimerization domains showed identical uptake, one region (residues 252-271, m/z 2260.154) within the dimerization domain subdomain of RelA had

increased uptake in the absence of the DNA-binding domain. Two overlapping peptides within the p50 dimerization domain also showed increased uptake, residues 283-298 (m/z 1863.734) and residues 283-308 (m/z 3002.286). Because a much larger difference in uptake was observed for the 283-308 peptide, it is possible to assign the changing region to residues 298-308 (Figure 7). These same regions did not show differences in the free NFκB constructs. It is interesting that the regions showing a difference in uptake corresponded to different structural regions within the dimerization domain subdomains of RelA vs. p50.

Discussion

The canonical and most abundant form of NFκB is the RelA-p50 heterodimer. Although the structures of the RHDs of each monomer are similar in architecture, comparison of the overall exchange within each RHD revealed that the RelA subunit exchanges more of its amides within 5 min than does p50. These results would suggest that the RelA homodimer may be less stable than the RelA-p50 heterodimer [17]. Despite this difference, the behavior of structural regions of each subunit was remarkably similar. Each showed marked protection upon DNA-binding in similar regions, and each showed increased exchange within similar regions of the dimerization subdomains. Each also showed decreased exchange throughout the entire DNA-binding subdomain upon IκBα binding. This result was striking because IκBα does not contact the DNA-binding subdomain at all in the crystal structure. The most likely explanation for such decreased exchange at-a-distance is long-range allostery. The global decrease in exchange throughout the entire DNA-binding subdomain of both the RelA and the p50 monomers was reflected in global stabilization to thermal challenge that was substantially stronger than the stabilization due to DNA binding.

Our HDXMS results also revealed regions of NFκB that exchanged more upon DNA binding as compared to free NFκB. All of these regions exchange less upon IκBα binding as compared to free NFκB. One of these regions is the NLS. It is very interesting that DNA binding causes a long-range allosteric increase in exchange of this region. This result suggests that when NFκB is bound to DNA, the NLS samples a larger conformational space than even in free NFκB. Such wide conformational sampling would promote a fly-casting mechanism [18] for the NLS to facilitate binding of an IκBα molecule resulting in more rapid stripping. Once IκBα is bound, the NLS caps the Ankyrin repeat domain of IκBα and is therefore expected to be protected from exchange, which is what was observed.

We previously used AWSEM-MD simulations to probe the molecular dynamics of NFκB during molecular stripping. We initially thought that IκBα simply bound to NFκB bringing the negatively-charged PEST region of IκBα close to the DNA resulting in electrostatic repulsion and weakening of the DNA binding. While this is part of the story, the simulations revealed a much more subtle effect in which binding of IκBα to the dimerization domains of NFκB caused the DNA-binding domains to twist relative to one another such that the DNA could no longer bind to both DNA-binding domains in the heterodimer [19]. Because the NFκB-IκBα complex could not be crystallized with both DNA-binding domains present, it was not possible to discover this allostery from x-ray crystallography alone. The HDXMS results are completely consistent with this proposed model although they report on internal dynamics rather than on whole domain motions. In fact, upon IκBα binding, we observed

large decreases in amide exchange indicative of global dampening of the internal dynamics of the DNA-binding domains despite there being no direct contact between the IκBα and these domains. While internal dynamics changes are distinct from a twisting and restricting of global motions of the DNA-binding domains, they are not inconsistent, and one might speculate that dampened internal dynamics may accompany the restricted global motion of the subdomains.

It is very interesting that the region within the dimerization domain of p50 that shows increased dynamics upon DNA binding is the same region that showed increased deuterium uptake in the IκBα-bound DNA-binding domain deletion construct. On the other hand, the region in RelA that showed increased dynamics upon DNA binding was residues 226-238, adjacent to the region that showed increased deuterium uptake in the IκBα-bound DNA-binding domain deletion construct. It is tempting to speculate that the proposed “twisting” of the NFκB heterodimer upon IκBα binding is reflected in these differences in amide exchange. Future work will seek to confirm this speculation.

Materials and Methods

Protein expression and purification

Homo sapiens $I\kappa B\alpha_{67\text{-}287}$ (IκBα) was expressed and purified as described[20]. Murine, N-terminal hexahistidine-$p50_{39–350}$/$RelA_{19–321}$ heterodimer (full-length NFκB) was co-expressed as described previously [21] and purified by nickel affinity chromatography and cation exchange chromatography (Mono S, GE Healthcare). Murine dimerization domain $p50_{248\text{-}350}$/$RelA_{190\text{-}321}$ (dimerization domain NFκB) was co-expressed and purified as described[22]. Immediately prior to experiments, IκBα (Superdex 75, GE Healthcare), dimerization domain NFκB (Superdex 75), and full-length NFκB (Superdex 200, GE Healthcare) were purified by size exclusion chromatography. NFκB was incubated in a 1.2-fold excess of IκBα, and the NFκB-IκBα complex was purified by size exclusion chromatography (Superdex 200). Protein concentrations were determined by spectrophotometry at 280 nm (NFκB $\varepsilon = 43760\ M^{-1}\ cm^{-1}$, IκBα $\varepsilon = 12950\ M^{-1}\ cm^{-1}$).

DNA sample preparation

A hairpin DNA sequence corresponding to the ten-nucleotide IFN-κB site (underlined) 5′-GGGAAATTCCTCCCCCAGGAATTTCCC-3′ (IDT Technologies) was dissolved in Milli-Q water to 1 mM.

Circular dichroism thermal denaturation

Circular dichroism (CD) thermal denaturation measurements were performed on an Aviv 202 spectropolarimeter (Aviv Biomedical) equipped with thermoelectric temperature control using a 0.2 cm path-length quartz cuvette. Individual proteins and complexes were purified by size exclusion chromatography in 10 mM NaH_2PO_4 pH 7.5, 150 mM NaCl,1 mM DTT, 0.5 mM EDTA immediately prior to analysis and diluted to 10 μM. A 1.2-fold excess of IFN-κB hairpin DNA was added to NFκB to generate the NFκB-DNA complex. Ellipticity was monitored at 225 nm as the temperature was increased from 25 °C to 80 °C with 0.5 °C

steps, an averaging time of 5 s, an equilibration time of 0.1 min, and a 1.5 °C/min rate of change.

The thermal denaturation curves were fit to the following equation:

$$y=\frac{y_{N+}m_N T+(y_D+m_D T)e^{[\Delta H_{vh}(1/T_m-1/T)/R]}}{1+e^{[\Delta H_{vh}(1/T_m-1/T)/R]}},$$

where y is the ellipticity signal, y_N (native) and y_D (denatured) are the baseline intercepts, m_N (native) and m_D (denatured) are the baseline slopes, T is the temperature, ΔH_{vh} is the van't Hoff enthalpy, T_m is the temperature of the transition point, and R is the gas constant[5].

Hydrogen-deuterium exchange mass spectrometry

Hydrogen/deuterium exchange mass spectrometry (HDXMS) was performed using a Waters Synapt G2Si equipped with nanoACQUITY UPLC system with H/DX technology and a LEAP autosampler. Individual proteins and complexes were purified by size exclusion chromatography in 25 mM Tris pH 7.5, 150 mM NaCl, 1 mM DTT, 0.5 mM EDTA immediately prior to analysis. The NFκB-DNA complex was prepared by an overnight incubation of NFκB in a ten-fold excess of the IFN-κB hairpin DNA. The final concentrations of proteins and complexes in each sample were 5 μM. For each deuteration time, 4 μL complex was equilibrated to 25 °C for 5 min and then mixed with 56 μL D_2O buffer (25 mM Tris pH 7.5, 150 mM NaCl, 1 mM DTT, 0.5 mM EDTA in D_2O) for 0, 0.5, 1, 2, or 5 min. The exchange was quenched with an equal volume of quench solution (3 M guanidine, 0.1% formic acid, pH 2.66).

The quenched sample was injected into the 50 μL sample loop, followed by digestion on an in-line pepsin column (immobilized pepsin, Pierce, Inc.) at 15°C. The resulting peptides were captured on a BEH C18 Vanguard pre-column, separated by analytical chromatography (Acquity UPLC BEH C18, 1.7 μM, 1.0 × 50 mm, Waters Corporation) using a 7–85% acetonitrile in 0.1% formic acid over 7.5 min, and electrosprayed into the Waters SYNAPT G2Si quadrupole time-of-flight mass spectrometer. The mass spectrometer was set to collect data in the Mobility, ESI+ mode; mass acquisition range of 200–2,000 (m/z); scan time 0.4 s. Continuous lock mass correction was accomplished with infusion of leu-enkephalin (m/z = 556.277) every 30 s (mass accuracy of 1 ppm for calibration standard). For peptide identification, the mass spectrometer was set to collect data in MS^E, ESI+ mode instead.

The peptides were identified from triplicate MS^E analyses of 10 μM IκBα, 10 μM full-length NFκB, and 10 μM dimerization domain NFκB, and data were analyzed using PLGS 2.5 (Waters Corporation). Peptide masses were identified using a minimum number of 250 ion counts for low energy peptides and 50 ion counts for their fragment ions. The peptides identified in PLGS were then analyzed in DynamX 3.0 (Waters Corporation). The following cut-offs were used to filter peptide sequence matches: minimum products per amino acid of 0.2, minimum score of 7, maximum MH+ error of 3 ppm, a retention time standard deviation of 5%, and the peptides were present in two of the three ID runs. After back-

exchange correction (~27%), the relative deuterium uptake for each peptide was calculated by comparing the centroids of the mass envelopes of the deuterated samples with the undeuterated controls following previously published methods [23]. The experiments were performed in triplicate, and independent replicates of the triplicate experiment were performed to verify the results.

Molecular Modeling

HDXMS data is best viewed and understood by displaying the extent of deuterium uptake on structural models. However, only partial structural models of NFκB are available from x-ray crystallography. To generate the full molecular models of the NFκB-DNA complex, we added RelA residues 292-321 corresponding to the NLS onto the crystal structure of NFκB(RelA-p50) bound to the IG/HIV-κB site DNA (PDB code 1LE9). To do this, we aligned the 1LE9 structure with the NFκB(RelA p50)-IκBα structure (PDB code 1NFI) by overlaying NFκB dimerization domains using LOVALIGN [24]. After the alignment, the NLS from 1NFI was manually added to 1LE9 and solvated in a TIP3P [25] water box with the AMBER molecular simulation package [26,27]. To allow the bonds and angles to relax and eliminate possible bad contacts, the complete and solvated model was submitted to the following refinement procedure using AMBER and the ff14SB forcefield: i) 1000 steps of energy minimization of the water molecules with the protein atoms restrained and ii) 2500 steps of energy minimization with no position restraints.

For the complete model of the NFκB(RelA-p50)•IκBα complex, neither the 1NFI nor the 1IKN pdb files contained the p50 DNA-binding domain and each represented a different portion of the IκBα structure. We started from a merged structure with a complete IκBα but incomplete p50 (dimerization domain only) that was generated in the Ghosh lab by merging structures 1NFI and 1IKN (NFIKN) and p50 DNA-binding domain back to the IκB-NFκB model (NFIKN, merged crystal structures from 1NFI and 1IKN). Next we manually added the p50 dimerization domain, (p50 residues 39-245) from the 1LE9 pdb file to the NFIKN structure. To do this, we aligned the two NFκB structures by overlaying the NFκB dimerization domains. Then the p50 DNA-binding domain from 1LE9 was added to NFIKB. Again, the complete model was solvated with TIP3P water molecules and refined as already described.

Supplementary Material

Refer to Web version on PubMed Central for supplementary material.

Acknowledgments

This work was supported by NIH grant P01GM071862 to EAK. KMR acknowledges support from the Molecular Biophysics Training Grant, T32GM008326.

References

1. Ghosh S, May MJ, Kopp EB. NF-kB and Rel proteins: Evolutionarily conserved mediators of immune responses. Annu Rev Immunol. 1998; 16:225–260. [PubMed: 9597130]
2. Hoffmann A, Natoli G, Ghosh G. Transcriptional regulation via the NF-kB signaling module. Oncogene. 2006; 25:6706–6717. [PubMed: 17072323]

3. Hoffmann A, Levchenko A, Scott ML, Baltimore D. The IkB-NF-kB signaling module: temporal control and selective gene activation. Science. 2002; 298:1241–5. [PubMed: 12424381]
4. Kumar A, Takada Y, Boriek AM, Aggarwal BB. Nuclear factor-kappaB: its role in health and disease. J Mol Med. 2004; 82:434–448. [PubMed: 15175863]
5. Consalvi V, Chiaraluce R, Giangiacomo L, Scandurra R, Christova P, Karshikoff A, Knapp S, Ladenstein R. Thermal unfolding and conformational stability of the recombinant domain II of glutamate dehydrogenase from the hyperthermophile Thermotoga maritima. Protein Eng. 2000; 13:501–507. [PubMed: 10906345]
6. Baeuerle PA. IkB-NF-kB structures: at the interface of inflammation control. Cell. 1998; 95:729–731. [PubMed: 9865689]
7. O'Dea EL, Barken D, Peralta RQ, Tran KT, Werner SL, Kearns JD, Levchenko A, Hoffmann A. A homeostatic model of IkappaB metabolism to control constitutive NF-kappaB activity. Mol Syst Biol. 2007; 3:111. [PubMed: 17486138]
8. Bergqvist S, Alverdi V, Mengel B, Hoffmann A, Ghosh G, Komives EA. Kinetic enhancement of NF-kappaB•DNA dissociation by IkappaBalpha. Proc Natl Acad Sci U S A. 2009; 106:19328–33. [PubMed: 19887633]
9. Alverdi V, Hetrick B, Joseph S, Komives EA. Direct observation of a transient ternary complex during IκBα-mediated dissociation of NF-κB from DNA. Proc Natl Acad Sci U S A. 2014; 111:225–230. [PubMed: 24367071]
10. Potoyan DA, Zheng W, Komives EA, Wolynes PG. Molecular stripping in the NF-κB IκB DNA genetic regulatory network. Proc Natl Acad Sci U S A. 2016; 113:110–115. [PubMed: 26699500]
11. Truhlar SME, Mathes E, Cervantes CF, Ghosh G, Komives EA. Pre-folding IkappaBalpha alters control of NF-kappaB signaling. J Mol Biol. 2008; 380:67–82. [PubMed: 18511071]
12. Trelle MB, Ramsey KM, Lee TC, Zheng W, Lamboy J, Wolynes PG, Deniz A, Komives EA. Binding of NFkB Appears to Twist the Ankyrin Repeat Domain of IkBa. Biophys J. 2016; 110:887–895. [PubMed: 26910425]
13. Jacobs MD, Harrison SC. Structure of an IkappaBalpha/NF-kappaB complex. Cell. 1998; 95:749–758. [PubMed: 9865693]
14. Huxford T, Huang DB, Malek S, Ghosh G. The crystal structure of the IkappaBalpha/NF-kappaB complex reveals mechanisms of NF-kappaB inactivation. Cell. 1998; 95:759–770. [PubMed: 9865694]
15. Croy CH, Bergqvist S, Huxford T, Ghosh G, Komives EA. Biophysical characterization of the free IkappaBalpha ankyrin repeat domain in solution. Protein Sci. 2004; 13:1767–77. [PubMed: 15215520]
16. Bergqvist S, Croy CH, Kjaergaard M, Huxford T, Ghosh G, Komives EA. Thermodynamics reveal that helix four in the NLS of NF-kappaB p65 anchors IkappaBalpha, forming a very stable complex. J Mol Biol. 2006; 360:421–434. [PubMed: 16756995]
17. Tsui R, Kearns JD, Lynch C, Vu D, Ngo KA, Basak S, Ghosh G, Hoffmann A. IκBβ enhances the generation of the low-affinity NFκB RelA homodimer. Nat Commun. 2015; 6:7068. [PubMed: 25946967]
18. Lätzer J, Papoian GA, Prentiss MC, Komives EA, Wolynes PG. Induced fit, folding, and recognition of the NF-kappaB-nuclear localization signals by IkappaBalpha and IkappaBbeta. J Mol Biol. 2007; 367:262–274. [PubMed: 17257619]
19. Potoyan DA, Zheng W, Ferreiro DU, Wolynes PG, Komives EA. PEST Control of Molecular Stripping of NFκB from DNA Transcription Sites. J Phys Chem B. 2016; 120:8532–8538. [PubMed: 27098223]
20. Dembinski HE, Wismer K, Balasubramaniam D, Gonzalez HA, Alverdi V, Iakoucheva LM, Komives EA. Predicted disorder-to-order transition mutations in IkBa disrupt function. Physical Chemistry Chemical Physics. 2014; 16:6480–6485. [PubMed: 24605363]
21. Sue SC, Cervantes C, Komives EA, Dyson HJ. Transfer of flexibility between ankyrin repeats in IkappaBalpha upon formation of the NF-kappaB complex. J Mol Biol. 2008; 380:917–931. [PubMed: 18565540]
22. Bergqvist S, Ghosh G, Komives EA. The IkBa/NF-kB complex has two hot-spots, one at either end of the interface. Prot Sci. 2008; 17:2051–2058.

23. Wales TE, Fadgen KE, Gerhardt GC, Engen JR. High-speed and high-resolution UPLC separation at zero degrees Celsius. Anal Chem. 2008; 80:6815–6820. [PubMed: 18672890]

24. Martínez L, Andreani R, Martínez JM. Convergent algorithms for protein structural alignment. BMC Bioinformatics. 2007; 8:306. [PubMed: 17714583]

25. Jorgensen WL, Chandrasekhar J, Madura JD, Impey RW, Klein ML. Comparison of simple potential functions for simulating liquid water. J Chem Phys. 1983; 79:926–935.

26. Case, DA., Darden, T., Cheatham, TE., 3rd, Simmerling, C., Roitberg, A., Wang, J., Duke, RE., Luo, R., Roe, DR., Walker, RC., LeGrand, S., Swails, J., Cerutti, D., Kaus, J., Betz, R., Wolf, RM., Merz, KM., Jr, Seabra, G., Janowski, P. AMBER14. University of California; San Francisco: 2015.

27. Case DA, Cheatham TE 3rd, Darden T, Gohlke H, Luo R, Merz KM Jr, Onufriev A, Simmerling C, Wang B, Woods RJ. The Amber biomolecular simulation programs. J Comput Chem. 2005; 26:1668–1688. [PubMed: 16200636]

Highlights

- Discovery of allostery in NFκB that runs between the two Ig-like subdomains of the Rel holomogy domain
- DNA binding induces allostery in NFκB, exposing the nuclear localization signal
- IκBα binding induces allostery in NFκB, consolidating the N-terminal DNA-binding domains

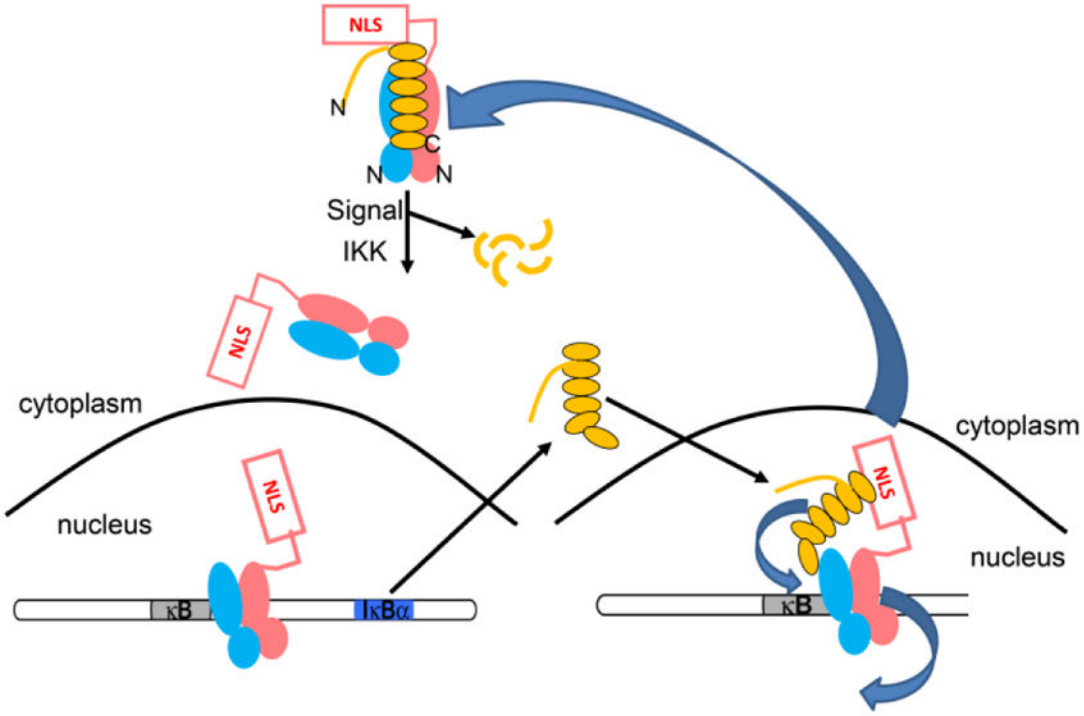

Figure 1.

IκBα regulates NFκB activity. *(A)* IκBα (yellow) sequesters NFκB (salmon and cyan) in the cytoplasm. The N- and C-termini of IκBα are labeled and the N-termini of the NFκB heterodimer are also marked. When an extracellular stress signal (e.g., LPS, TNFα) is received, IκBα is phosphorylated by IKK, ubiquitinated, and degraded, thus unmasking the NFκB nuclear localization signals (NLS) whereupon it enters the nucleus and binds to κB DNA sites. *(B)* One of the genes under control of the κB promoter is IκBα, so newly synthesized IκBα then enters the nucleus, strips NFκB from DNA, and exports NFκB out of the nucleus.

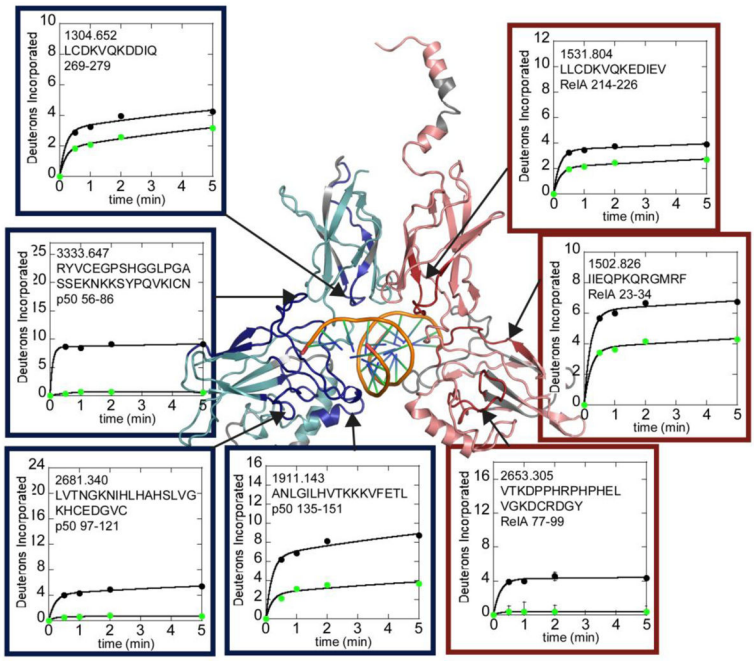

Figure 2.

HDXMS analysis of free NFκB (black circles) compared to DNA-bound NFκB (green circles). The interface regions within RelA (salmon) and p50 (cyan) in the NFκB heterodimer that are protected upon DNA binding are shown on a model of the NFκB-DNA complex. Protected regions of RelA are colored red and protected regions of p50 are colored dark blue. Regions of each protein that were not covered in the HDXMS analysis are grey. The deuterium uptake plots are positioned near and arrows point to the corresponding region of the structure.

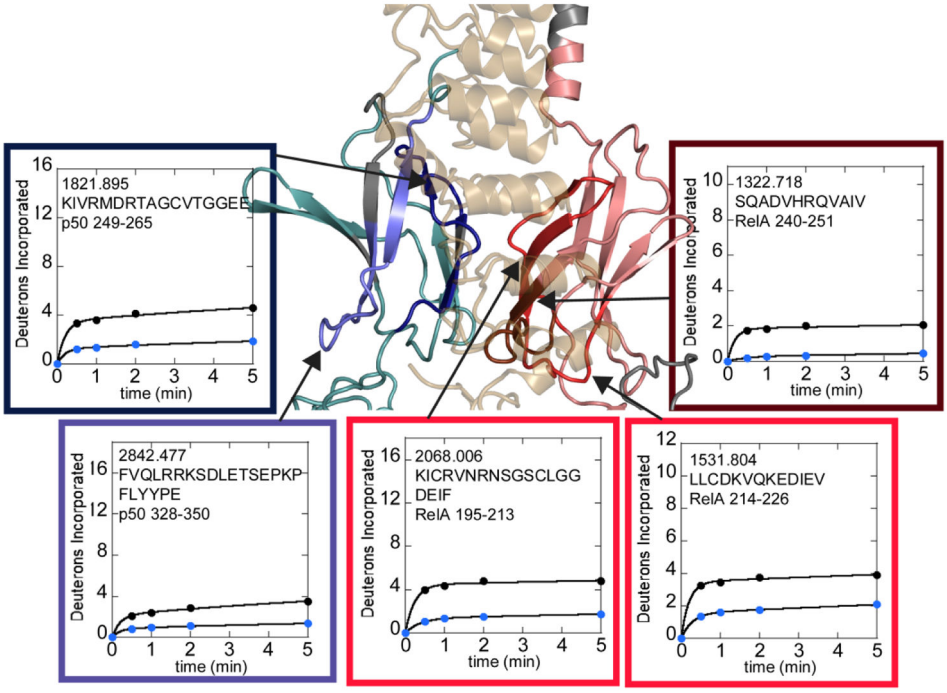

Figure 3.

HDXMS analysis of free NFκB (black circles) compared to IκBα-bound NFκB (blue circles). The interface regions within the dimerization domain subdomains that are protected upon IκBα binding are shown on a model of the NFκB-IκBα structure. RelA is shown in salmon with protected regions in hues of red. Only the dark red region is directly contacting IκBα. P50 is shown in teal with protected regions in hues of blue. Only the dark blue region is directly contacting the IκBα. Regions of each protein that were not covered in the HDXMS analysis are grey. The deuterium uptake plots are positioned near and arrows point to the corresponding structural region. The plots are boxed with colors similar to those used to denote direct and indirect protection on the structure.

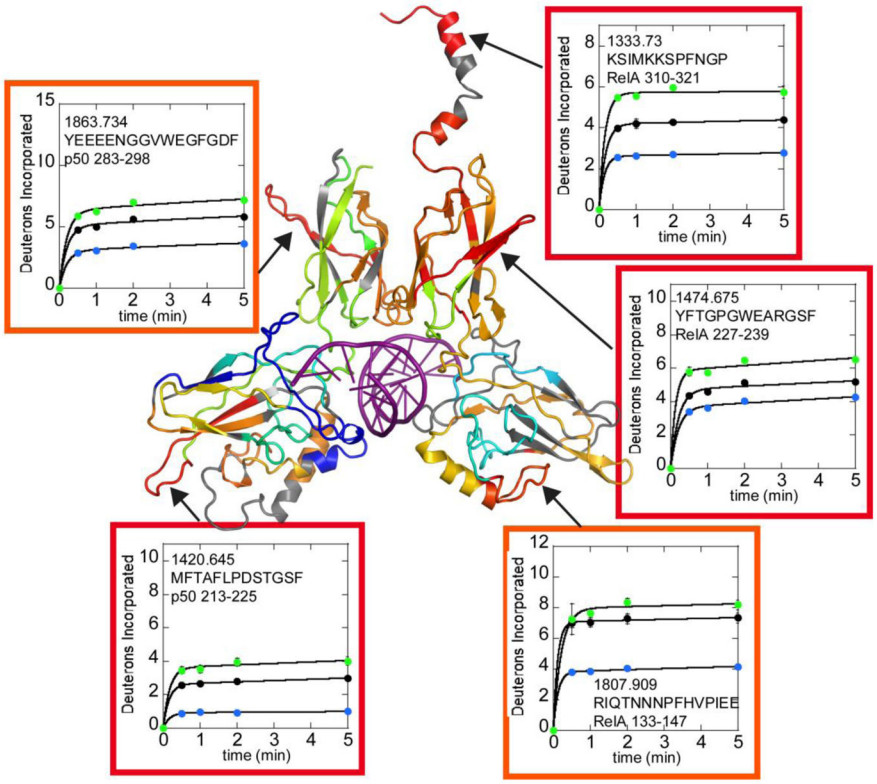

Figure 4.

Selected HDXMS uptake plots of regions of NFκB that exchange more upon DNA binding are plotted with free NFκB (black circles) vs. DNA-bound NFκB (green circles) or IκBα-bound NFκB (blue circles). The corresponding regions within NFκB are shown on a model of the DNA-bound NFκB (RelA-p50) structure. The model is colored according to a rainbow scale (blue-green-yellow-orange-red) representing the difference in fractional deuterium uptake between NFκB in complex with DNA as compared to NFκB alone. Boxes around each plot match to the color of the corresponding region in the structure. Red corresponds to 15% higher exchange in the NFκB-DNA complex and blue corresponding to 30% lower exchange in the DNA-bound form. The deuterium uptake plots are positioned near the corresponding structural regions and are also marked by arrows.

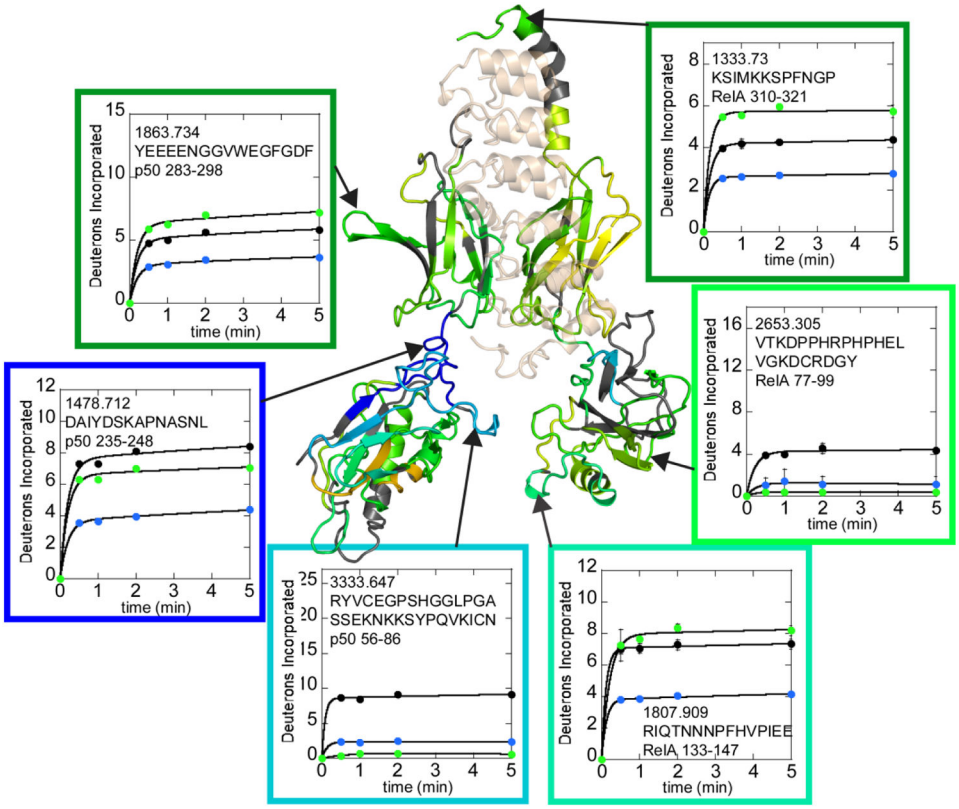

Figure 5.

Selected HDXMS uptake plots of free NFκB (black circles) vs. IκBα-bound NFκB (green circles) or IκBα-bound NFκB (blue circles) showing some of the regions within NFκB that exchange less when IκBα is bound. The IκBα-bound NFκB (RelA-p50) structure and boxes around each plot are colored according to the same rainbow scale with the same upper and lower bounds as that used in Figure 4. The deuterium uptake plots are positioned near the corresponding structural regions and are also marked by arrows.

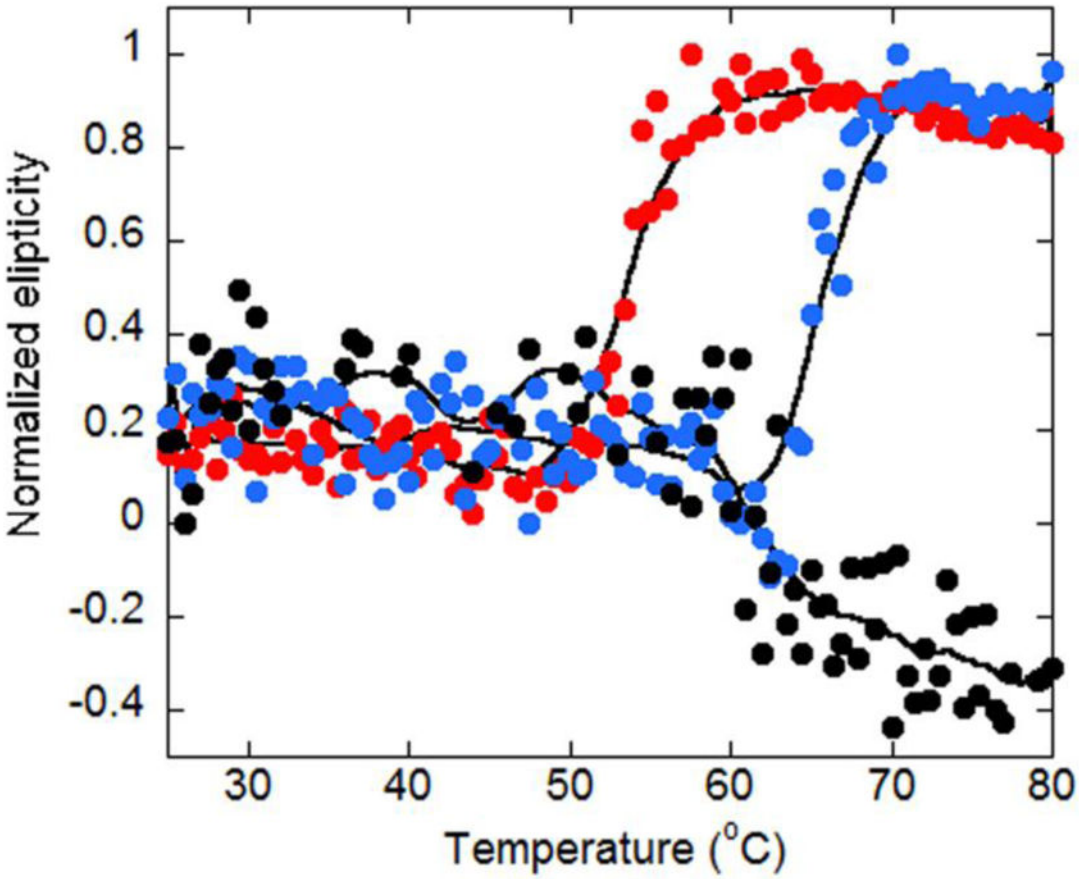

Figure 6.

Thermal melting curves were determined by circular dichroism monitoring the signal at 225 nm for NFκB alone (red circles), DNA-bound NFκB (blue circles) or IκBα-bound NFκB (black circles). The normalized CD signal at 225 is plotted against increasing temperature. The thermal denaturation of NFκB, IκBα, and their complexes is irreversible.

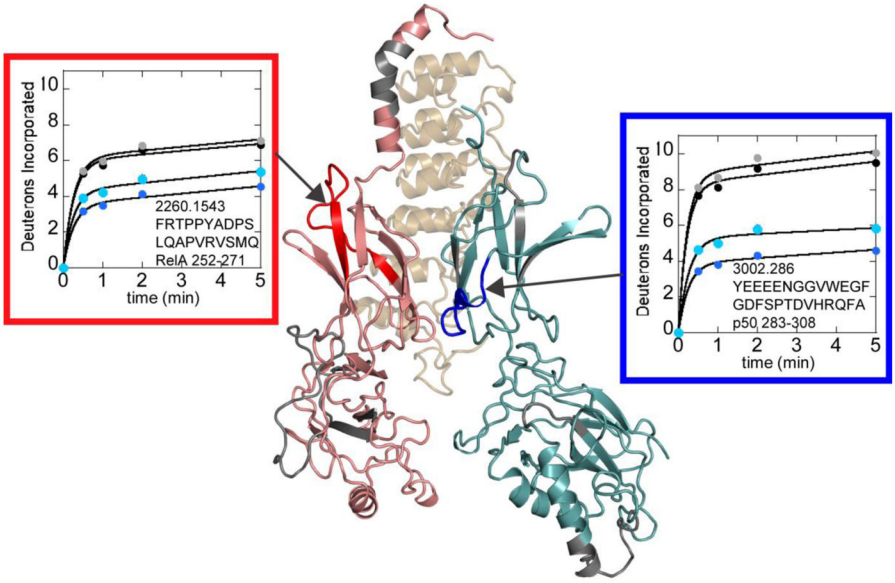

Figure 7.

Comparison of the deuterium uptake into full-length NFκB in complex with IκBα (blue) vs. the deuterium uptake into the DNA-binding domain deletion NFκB construct in complex with IκBα (cyan) revealed regions within the dimerization domain subdomains that had increased deuterium uptake in the deletion construct. These same regions did not show differences in free NFκB (full-length, black; DNA-binding domain deletion construct, grey). The difference in uptake was observed in different dimerization domain subdomain structural regions in RelA (red) vs. p50 (blue). The structural model is shown rotated 180° about the y axis compared to that shown in Figures 3 and 5 to more easily view the regions of interest.